

A Passive Islanding Detection Technique Based on Susceptible Power Indices with Zero Non-Detection Zone Using a Hybrid Technique

Mr. Ashwin K V^{1*}, Mr. Venkata Satya Rahul Kosuru², Mr. Sridhar S³, Mr. P. Rajesh⁴

Submitted: 08/11/2022

Accepted: 10/02/2023

Abstract: In the power system, incorporated distributed energy resources (DERs) bring the benefits of environmental, economic and technical. In addition to these benefits, it elevates some technical concerns when the penetration level of DERs is high. The major issues are islanding detection and it is necessary for equipment protection and personal safety. In this research, the phase angle of positive sequence voltage (PAOPSV) proposed a passive islanding detection scheme. The proposed hybrid method is the combined performance of dwarf mongoose optimizer (DMO) and random forest algorithm (RFA), hence commonly called as DMO-RFA method. From the strict analysis of 13 different factors, the PAOPSV is selected. In addition to this, for islanding in solar photovoltaic (SPV) based distributed generation (DG) system. The comparative analysis shows that among all other parameters, the PAOPSV has better accuracy and sensitivity for islanding parameters. In order to verify the efficiency of proposed method, a comprehensive case study consider all worst-case scenarios, which is accomplished the differentiates islanding events from the non-islanding events, like load, motor, capacitor, various fault type switching. The proposed system is implemented on MATLAB/Simulink, and the proposed work is performed on Intel Core 2 Quad CPUQ6600 at 2.40 GHz using 2 GB random access memory (RAM), MATLAB R2013a (8.1.0.604) 32-bit and Version 3.7.2.

Keywords: *Islanding detection, Distributed Energy Resources, PAOPSV, Non-islanding detection, Dwarf Mongoose Optimization (DMO), and Random Forest Algorithm (RFA).*

1. Introduction

To meet the load demands, the distributed energy resources play an important role. Generally, distributed energy resources are the generation units of small scale and it is often referred as distributed generation (DG) that contains mini-hydro's turbines, biomass, wind farms, solar plant, geothermal and fuel cell energies [1]. In the power system, the topological trends are introduced by the installation of distributed generation units into utility. From centralized to decentralized generation, the configuration type of power system is altered by these changes [2]. In the power system, the combination of DG units in utility introduces some positive changes, like increase in system flexibility, maximize the effectiveness of system and power loss reduction [3]. Apart from these positive impacts, there are some technical issues, like islanding, coordination problem of protection, false tripping, safety, stability, and trustworthiness of the system, voltage regulation and

security of the system are also introduced by the combination of distributed generation units on utility [4]. One of the major issues is islanding detection. Local loads are continuously increased by distributed generations (DGs) in islanding detection to interact with grid supply interruption. The technical issues like load power quality (PQ) issues; safety issues for workers are caused by the uninvited condition named islanding [5]. Islanding identification is divided into two groups, the first one is remote technique in which the utility side, and the measurements are carried out. Second technique is local technique from which the measurement is taken place in the distributed generation side. Regarding the non-detection zone (NDZ), the performance of every technique is described. The region that cannot be detected by the islanding detection is the NDZ.

For communication among utility and DG, a link is needed in remote schemes. These schemes have the advantages of high reliability and non-zero detection zone. But, the major disadvantage of this scheme is the high implementation cost [6-8]. Further, the local methods are classified into 2: active and passive. It operates on principle of local parameter measurements such as voltage, frequency, Total harmonic distortion (THD), and passive method at the point of interconnection (POI) [9]. The important objective of the passive method is relay transmits a trip signal to the breaker of distribution unit, if

¹Research Scholar, University of Cincinnati, Ohio, USA

¹Email: ashwin.venkit@gmail.com

²Research scholar, Lawrence Technological University, Michigan, USA

²Email: venkosuru@gmail.com

³Associate Professor, Department of Electrical and Electronics Engineering, M S Ramaiah Institute of Technology, Bangalore, India

³Email: sridhars@msrit.edu

⁴Department of Electrical and Electronics Engineering, Anna University, Tamil Nadu, India

⁴Email: rajeshkannan.mt@gmail.com

¹*Corresponding author email: ashwin.venkit@gmail.com

the measured parameters exceed the defined threshold value [10-12]. The simple execution and bearing without power quality issues are advantages of passive technique [13]. Anyhow, the major drawbacks are the large non-detection zone [NDZ] and threshold selection [14, 15]. Some passive methods use improved work for islanding detection and signal processing technique for NDZ reduction depends on some advanced intelligence methods. In [16], the schemes based on Random forest classifier, Naive Bayesian classifier, fuzzy logic, decision tree, artificial neural network have been introduced. Depending on s-transform (ST), wavelet transforms (WT) and wavelet packet transforms (WPT), few research analyst presented in the established technique [17]. In the abnormal condition, to access the parameters deviations, the disturbing signals are introduced into the system in an active technique. In the mode of grid-tied, there is no remarkable difference in the parameters. But, this parameter has some notable changes in islanding mode. The active methods have almost minimal NDZ when compared to passive methods [18- 20]. With regards to the addition of distributed signals, the active technique produces degradation of PQ distribution system. A hybrid method is the joint execution of active and passive islanding technique. Figure 1 shows the Organization of the research work.

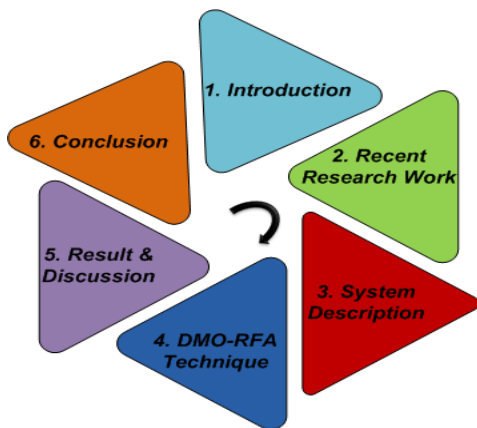


Fig. 1: Organization of research work

2. Recent Research work

Numerous research works previously depicted in literatures based on islanding detection problems on DG using various design and features. Few works are mentioned below.

For inverter-based DG units, M. Seyedi *et al.* [21] have presented an islanding detection technique named hybrid islanding detection. Generally, when power mismatches were almost zero, a passive islanding detection may fail. As a result, another common problem was difficulty of setting the threshold. In order to resolve these issues depending on combination of rate of change of active power (ROCOAP) and rate of change of voltage

(ROCOV), a novel islanding detection system was introduced. In the distribution networks (DNs) with distribution generation units, A.S. Fontova *et al.* [22] have introduced a technique for detecting unintentional islanding operations (IOs), which eliminates the NDZ. For an inverter-fed distribution generation (DG) state, by taking the merits of active and passive systems, the hybrid method achieves zero NDZ. In the introduced method, the passive-based part considers setting with low thresholds and whenever they exceeds it will be activated. The DC microgrids (MGs) were receiving a wide support in modern power grids, owing to increased usage of DC loads, increased efficiency, and integration of distributed generators and decreased conversion stages. For both DC and AC MGs, islanding detection was a major issue. For DC MGs based on cumulative sum of superimposed impedance (CSOSI), a novel passive islanding detection scheme (IDS) was introduced in B. Choudhury and P.Jena [23]. Here, for an islanding condition at distributed generation terminals, the current and voltage terminals were collected to examine a DC MG response. To detect islanding phenomena, the variations in CSOSI were measured and the superimposed impedance (SI) and cumulative sum of superimposed impedance were calculated. In the smart distribution systems, the renewable-based DERSs(R-DERS) were presented by Omar.A *et al.* [24] was extensively used. In spite of all the advantages of R-DERS, the presented method also introduces few operating challenges, like various protection issues, reverse power flow, and un-intentional islanding. Around the electrical power systems because of some unpredictable faults, an island or multiple islands were made.

The reliability of renewable energy sources (RESs) can be increased by the development in solar photovoltaic (PV), wind turbine and fuel cell field was integrated with high power electronics was established by A.Khair *et al.* [25]. To meet out the growing demand of load, the environmental advantages of RESs were switch over for various distributed generations. Generally, after the occurrence of islanding all distribution generations (DGs) need to be disconnected immediately. Every distribution generations should provide suitable island detection technique, proceeding to the combination of distribution generations to main electrical grid. From the upstream network, when distribution generations (DGs) were electrically disconnected islanding on system. To ensure the power quality requirements and maintenance safety, the islanding condition should be detected effectively. For identifying the islanding operating mode of grid-connected PV systems (GCPVSS), R.B.Jafarabadi *et al.* [26] have suggested a novel high PQ maximal power point tracking (MPPT) based technique. In the suggested 2-level model under suspicious condition, a disturbance was inserted into

the maximum power point tracking that was identified through a passive criterion. In islanding state, the disturbance drift the output voltage beyond the minimal standard set, on the other hand at the network presence was negligible. S. Kulkarni et al. [27] have presented an islanding detection and automatic mode switching with an improved droop controlled method. Among the distribution generations (DGs), the alteration in the traditional droop brings about the load proportionate to share the power capacity. The virtual impedance was executed for microgrid to increase the sharing of reactive power and to mitigate the circulating currents in stand-alone mode operation. Furthermore, the operation of microgrid, a modified Park synchronous reference frame fed phase-locked loop (PSRF-PLL) was presented. Here, the presented PLL always maintain the phase locking error almost zero and it leads to proper locking with mitigated complexity and it also have an advantage of simple construction. In the loop platform, with real time hardware, the control system's performance in MG was verified.

2.1. Background of the research work

The literature review demonstrates that various islanding techniques are used to detect islanding. One of the islanding detection approaches is the hybrid islanding detection that has a greater advantage of not interrupting the power supply in the island even during grid disturbance. This technique helps to supply and restore the system power in various power plants. When compared to restoration of the whole system, the island restoration is easy. Besides these advantages, this technique has disadvantages, like high cost and its capacitor bank must be large enough to cause changes in voltage. In order to design controller for PV system, MPPT algorithms are used. This algorithm has an advantage of working optimizing voltage and DC load in the PV system, increases charging efficiency and generates maximum power. On the other hand, it has few demerits, like short life span, expensive and large size. In micro grid, the incorporation of DER has many advantages, such as improved quality of service, high reliability and it can sell power bank to the grid so the electricity cost will be less. But, reducing the electricity is the most challenging one and also the operating utilities must invest in the infrastructure to maintain the grid. The PSRF-PLL islanding technique is widely used implementing operation of micro-grid that has advantages, like simple construction, high performance and reduced complexity. A challenging part of this technique is to maintain the phase-locking error almost zero.

3. System description

The islanding is an important security issues in grid-connected photovoltaic system. By the condition of islanding, the photovoltaic system and grid are affected in distributed generation. Further, an islanding situation, the grid frequency and voltage is not stable. By this condition, under the mode of islanding, the fault is recovered from the phase reference with end-point values from which the circuit breaker (CB) is connected among phase and PCC. Further, distributed generation still delivers power with local load if the circuit breaker does not open the circuit [28-30]. The islanding activity is occurred due to uncommon grid interference and these different situations are occurred based on the condition of equipment disappointment, short-circuit and voltage shutdown.

3.1. Mathematical model of distributed generation (DG) unit

In photovoltaic based system of DG, the islanding consists of 3 principle segments. For eg, boost converter of direct current to direct current, solar photovoltaic array, and a photovoltaic inverter along with its filter [31, 32]. Thus, the equation of 3 important areas are explained in the below steps,

3.1.1. Photovoltaic array model

It is a straightforward converter that is transformed into power through a photovoltaic cell. Based on the material of the cell, it practically distributes a constant open circuit voltage though current I_{PV} (cell) is running with the related load based on the energy of light (photons). Hence, it is measured in the below equation,

$$I_{PV(\text{cell})} = I_{ph} - I_o \left[\exp \left\{ \frac{\gamma(V_{PV} + I_{PV}R_s)}{\eta_k T} \right\} - 1 \right] - \frac{V_{PV} + I_{PV}R_s}{R_p} \quad (1)$$

By embedding the factors m, n, the eqn (1) is calculated to acquire eqn for the array of photovoltaic. Thus, it is expressed in the below eqn,

$$I_{PV(\text{array})} = mI_{ph} - mI_o \left[\exp \left\{ \frac{\gamma(V_{PV(\text{array})} + I_{PV(\text{array})}R_s(n/m))}{n\eta_k T} \right\} - 1 \right] - \frac{V_{PV(\text{array})} + I_{PV(\text{array})}R_s(n/m)}{R_p(n/m)} \quad (2)$$

The I_{ph} subject to the parameters like solar irradiance and ambient temperature. Thus, it is expressed below,

$$I_{ph} = I_{sc} \frac{I_{rrad}}{I_{rrad}^*} \left[1 + (T - T_{ref}) \times k_i \right] \quad (3)$$

3.1.2. Direct current to Direct current model

Here, it is necessary to convert direct current to direct current to get the ideal bus voltage of direct current. The

inductor (L), capacitor (C), and passive elements of converter is calculated below,

$$L = \frac{V_i(V_o - V_i)}{\Delta I_i f_s V_o} \quad (4)$$

$$C = \frac{I_o D}{\Delta v f_s} \quad (5)$$

A duty-cycle D is expressed below,

$$D = 1 - \left(\frac{V_i}{V_o} \right) \quad (6)$$

From eqn (6), ΔI_i as input current up to ten percent, ΔV specifies boost-converter output voltage upto three percent.

3.1.3. Inverter model of PV

Here, the voltage of direct current is transformed into the voltage of alternating current through 3-phase converter of voltage source. The 6 insulated gate bipolar transistors (IGBTs) are categorized into 2-level photovoltaic inverter. The equivalent photovoltaic inverter method for voltage equation is measured using additional eqn in the frame of stationary and rotating,

$$v_c = R_f I_s + L_f \frac{d(I_s)}{dt} + v_s \quad (7)$$

$$v_{cdq} = R_f I_{sdq} + L_f \frac{d(I_{sdq})}{dt} + v_{sdq} + j\omega L_f I_{sdq} \quad (8)$$

Real and reactive power are computed below,

$$P = \frac{3}{2} \text{Re}\{v_s I_s^*\} \quad (9)$$

$$Q = \frac{3}{2} \text{Im}\{v_s I_s^*\} \quad (10)$$

3.2. Proposed Method for Islanding Detection on DG Systems

To identify and categorize the events of islanding and non-islanding in DGS, 3 important areas are used, for e.g., Feature Extraction, Dataset Generation, Detection, and Classification. The negative sequence component of PCC voltage is eliminated under the dataset generation method. In order to remove the negative sequence component, the voltage signal is examined as well as the non-stationary signals are passed with sequence analyzer [33-35]. Structure of proposed system portrays on figure 2.

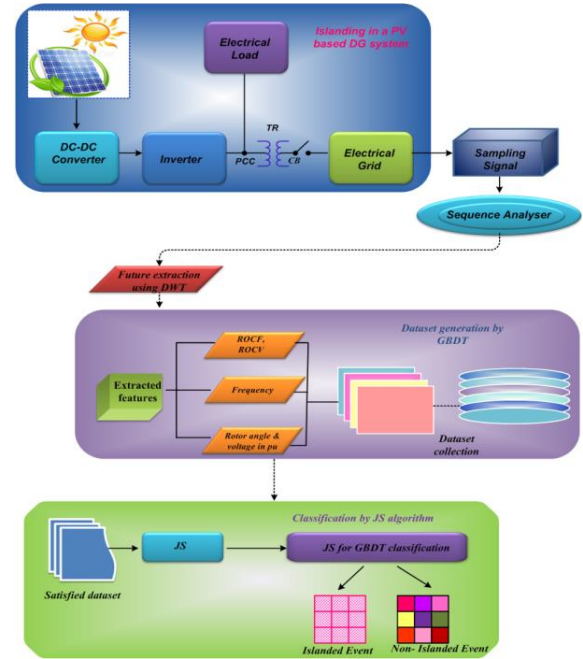


Fig. 2: Structure of proposed system

The main objective of proposed method is to model an effective method by embracing the joined FATOCSSO system to deal with islanding detection [36-38]. Initially, a dataset subject is created with negative sequence voltage signal in the data acquisition process. From the voltage signal, the five feature combination is separated, for instance, voltage in pu, rotor angle, rate of change of voltage and frequency. In feature extraction phase, the excess data are removed. In addition to this, a hybrid FATOCSSO is attuned to find and categorizes the detection of islanding and non-islanding.

3.2.1. Data generation

To give intellectual types of generous data based on the difference among the events of non-islanding and islanding, a large number of these occasions are illustrated in the test law [39]. The mismatches of active and reactive power are small (0 to30%) and large power mismatch (30-100%). At every bus, the non-islanding events integrates capacitor bank switching, DER tripping, motor switching, load switching, 3 phase and single phase-to-ground and phase-to-phase fault.

3.2.2. Feature Extraction

It is employed after the method of dataset generation to gather the voltage signal features in order to detect defects on DG system (DGS). To create framework at the middle of islanding period, the load and DG are used [40- 42]. When current is infused into or through utility, at that point immediately all the sides are interfered and then the distribution generation starts to maintain a load of small or large. Similarly, the angle for a reference and the terminal voltage are influenced. On the other hand, additionally the

change in voltage cycle time shows the adjustment in frequency. Taking the standard deviation (SD) into sliding data-window possessing ΔT as width, the 5 features are improved from the 5 variables. For example, by taking the SD in sliding data window to possess ΔT as width, a feature from $s(t)$ signal from the 5 variable is separated. By following this methodology, five network variables, the five features, like capacitor switching, load switching, etc., are extracted under the middle of non-islanding and islanding situation. Thus, these 5 features are mathematically expressed in equation (11):

$$\sigma_v = std\{v(\tau); \quad \tau \in [t - \Delta T, t]\} \quad (11)$$

$$\sigma_f = std\{f(\tau); \quad \tau \in [t - \Delta T, t]\} \quad (12)$$

$$\sigma_\delta = std\{\delta(\tau); \quad \tau \in [t - \Delta T, t]\} \quad (13)$$

$$\sigma_{pv} = std\left\{\frac{dv(\tau)}{dt}; \quad \tau \in [t - \Delta T, t]\right\} \quad (14)$$

$$\sigma_{pf} = std\left\{\frac{df(\tau)}{dt}; \quad \tau \in [t - \Delta T, t]\right\} \quad (15)$$

Also, the feature vector is calculated below,

$$x = [\sigma_v \ \sigma_f \ \sigma_\delta \ \sigma_{pv} \ \sigma_{pf}]^T \quad (16)$$

Here, T specifies the operator of transpose.

4. Proposed DMO-RFA Technique

4.1. Dwarf Mongoose Optimization (DMO)

In a large territory, the dwarf mongoose accepted a semi nomadic way of life is more than enough to carry the entire group. Over-exploitation of a particular is prevented by this nomadic character and it also checks the whole territory exploration as the visited sleeping mound is not formerly returned [43, 44].

Step 1: Initialization

Initializing the input parameter like current, frequency and voltage

Step 2: Random Generation

The input parameters are chosen randomly.

Step 3: Fitness evaluation

It is determined from objective function. The objective function is, $E = [V * -V]$ & $E = [I * -I]$. Where, E specifies error function of system.

Step 4: Generally, babysitters are certain number of mongoose population, which is the mixture of males and females. Until the group restores at evening or midday, the babysitters remains young. In exploitation phase, within

the group the babysitters are swapped for the first to forage.

Step 5: Stopping criteria

Check the stopping criteria. If the best value of voltage, current and frequency are defined then stop the process or repeat the process.

4.2. Random Forest Algorithm (RFA)

RFA is the ensemble machine learning process that incorporates the method of prediction. The hyper parameters in RFA consist of 2 types: (1) count of splits on subset and (2) count of trees on forest [45]. Meanwhile, 2 difficulties are noted. At first complexity, the training samples are chosen randomly in order to select finest sequence. At second complexity, the fact that no clipping energy is used in this technique and it shows that every tree in the forests is a maximum number of trees. Depending on the historical dataset, the Random Decision Forest (RDF) effectively forecasts the load demand in the proposed method. Figure 3 displays the structure of RFA.

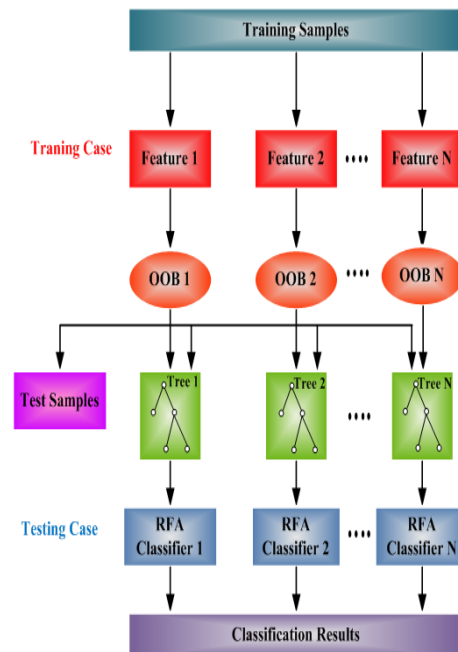


Figure 3: Structure of the RFA

Step 1: The output of dwarf mongoose optimization (DMO) is given as the input for Random Forest Algorithm (RFA) i.e. the output voltage, frequency and current.

Step 2: The classifier technique of random decision forest is formed by the combination of decision trees. Primarily, to create the decision tree from the forest Y number of trees are considered, which forms a combination of $Y = \{x_1(t), x_2(t), \dots, x_n(t)\}$ and every combinations are called bootstrap samples.

Step 3: A Random decision forest is trained depending on input and target. Here, only a few input variables are given

by every tree as well as it generates Z-output (one for each tree). In this, the last optimum outcome is acquired depending on maximal vote. The flowchart of RFA portrays on figure 4.

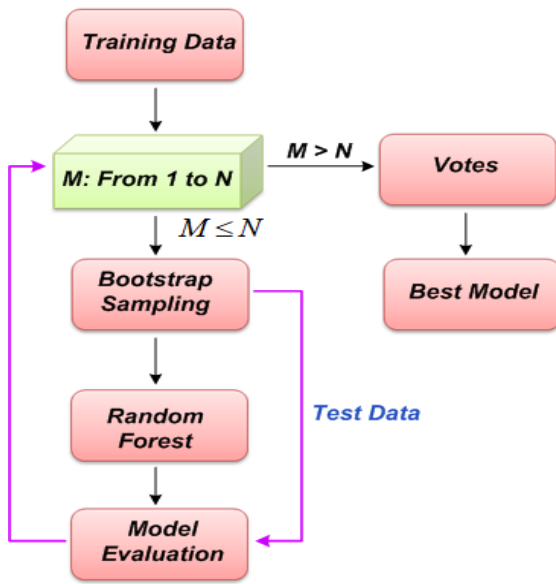


Fig. 4: Flowchart of RFA

Step 4: By analyzing the VI, the RDFs of the input variables are ranked in the process of prediction. The VI is identified by relating prediction error using data term of Out-Of-Bag (OOB). As shown in equation (7), the out-of-bag error target is expressed as below,

$$OOB_{error} = Z^{RDF(tr)} - Z^{RDF(out)} \quad (17)$$

Each sample control of different datasets improves the RDFs model. The number of separations is selected randomly in each node for making the binary rule. The RMSE is generated to forecast the finest split and the errors in RMSE are compared to out-of-bag data.

Step 5: The VI is calculated to increase the prediction accuracy. At this time, in each data, the on-of-bag error is designed and under fitting time over the forest these errors are averaged. Subjecting to OOB error difference, after training process, the variable importance (VI) of every data is determined before and after permutation over all trees. By using equation (8), the variable importance can be determined.

$$V_i^{(tr)} = \frac{1}{T} \left(\frac{\sum_{x \in \phi^{c(tr)}} I(l_b = C_a^{tr}) - \sum_{x \in \phi^{c(tr)}} I(l_b = C_{a,\pi}^{tr})}{\phi^{c(tr)}} \right) \quad (18)$$

whereas $\phi^{c(tr)}$ specifies OOB trail-specimen for peculiar tree, tr represents number of tree, T specifies net count of tree, for every trail specimens. $C_a^{(tr)}$, $C_{a,\pi}^{(tr)}$ indicates the predicted classes, X_a represents sample value, the count of

trail-specimens per tree leave in forest is indicated as a, b . The accuracy is maximized, only if the VI lessens there is a decrease in accuracy. By using the density model of cluster analysis method, the number of items similar to the item in the VI computation is partitioned. From the training dataset, the unfulfilled demands of load are predicted based on clustering response, then unsatisfied load demand is detected in this technique is detached and interchanged.

Step 6: In this step, after checking the stopping criteria, if yes then it will detect the islanding mode or non-islanding mode else go to step 3.

5. Results and Discussions

The efficiency and effectiveness of proposed DMO-RFA technique are defined under three main methods, data generation, feature extraction, and island and non-island cases of DG. The simulation outcomes achieved as proposed DMO-RFA method are related to existing methods like Dragonfly Algorithm (DFA) [46], Firefly Algorithm (FF) [47] and Gravitational Search Algorithm (GSA) [48]. The proposed method is experimented in voltage drop on islanded constraints, voltage rise at islanded constraints, voltage drop originated by disturbances, voltage rise originated by disturbances, swelling transient and synchrony. The performance of the proposed system is evaluated with MATLAB/Simulink platform. The brief explanations of test cases are described at below section.

5.1. Voltage Drop on Islanding Condition

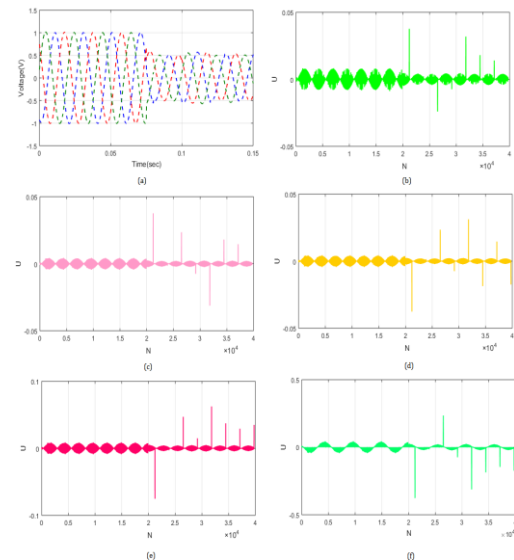


Fig. 5: Voltage drop under islanding constraints (a) 3-phase voltage (b) Scale 1 (c) Scale 2 (d) Scale 3 (e) Scale 4 (f) Scale 5.

Figure 5 demonstrates the voltage drop across the island in PCC under several levels of transition coefficients. Figure 5(a) shows the DG 3-phase voltage generated among time intervals from 0 to 0.15 sec. On this graph, 3-phase voltage is symmetrical and unity beyond 0.05 seconds, after which, at a time interval of 0.07 seconds, the voltage is suddenly reduced with 0.5 V that is maintained until the end of system operation. Fig. 5(b–f) demonstrates Voltage drop across the PCC in dissimilar levels of transition coefficients ranging from 1 to 5. The sampling point implies $4 \times 10^4 N$ and voltage drop happens among $2 \times 10^4 - 4 \times 10^4 N$ sampling points with its accurate time period.

5.2. Voltage Rise on Islanding Condition

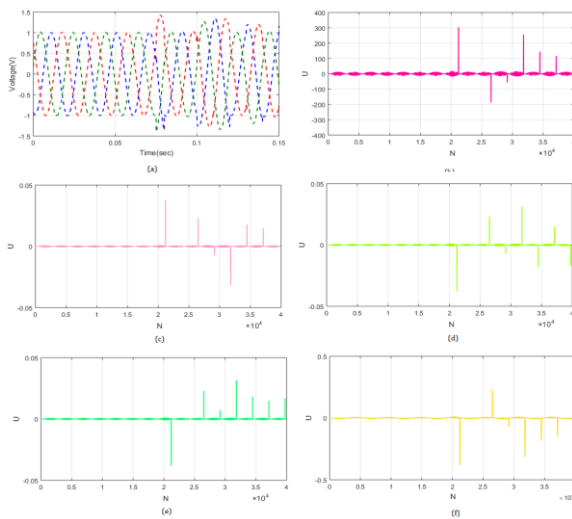


Fig. 6: Voltage rise under islanding constraints (a) 3-phase (b) Scale 1 (c) Scale 2 (d) Scale 3 (e) Scale 4 (f) Scale 5.

Figure 6 shows the island voltage rise on PCC in dissimilar scales of transition coefficients. Figure 6(a) portrays the 3-phase voltage. The phase voltage is balanced as well as unity is maintained beyond time interval of 0.05 sec. This phase voltage is suddenly raised at a time interval of 0.07 sec and fluctuates until the end of system operation. Figure 6(b–f) demonstrates island voltage rise on PCC under dissimilar levels of transition coefficients at scale 1 to 5. The voltage increase on PCC has occurred among sample points of $2.1 \times 10^4 - 4N$ using the time interval from 0 to 4×10^4 s.

5.3. Voltage Sag under Islanding Condition

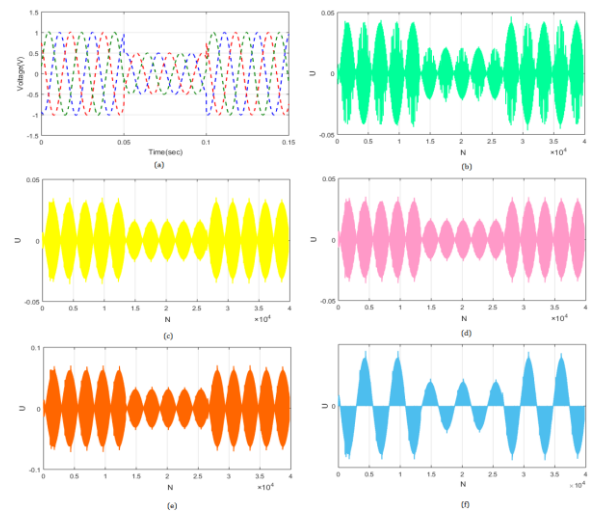


Fig. 7: Voltage Sag caused by disturbances (a) 3-phase (b) Scale 1 (c) Scale 2 (d) Scale 3 (e) Scale 4 (f) Scale 5

The voltage sag due to different scales of disturbances portrays on Figure 7. Figure 7(a) shows the 3-phase DG voltage. Voltage is balanced and unity through first time step from 0-0.05 seconds and 0.1-0.15 seconds. The voltage sag occurs at a time interval of 0.05 to 0.1 sec. Fig. 7(b) portrays voltage sag caused by perturbations in the transformation coefficients at various magnitudes at scale 1. Here, the voltage drop occurs at $1.4 \times 10^4 N$ to $2.7 \times 10^4 N$ at sample points. Fig. 7(c) portrays voltage sag due to disturbances under scale 2. Here, the voltage drop happens among the sampling from 1.4×10^4 to $2.7 \times 10^4 N$. Figure 7(d) illustrates voltage sag due to disturbances on scale 3. Here, the voltage drop occurs among sample points ranges from 1.4×10^4 to $2.7 \times 10^4 N$. Figure 7(e) portrays voltage drop due to disturbances under scale 4. Here, the voltage drop between 1.4×10^4 to $2.7 \times 10^4 N$ sample points occurs. Fig 7(f) portrays voltage sag due to disturbances on scale 5. Thus, the voltage sag occurs among sampling points from 1.4×10^4 to $2.7 \times 10^4 N$.

5.4. Voltage Swell under Islanding Condition

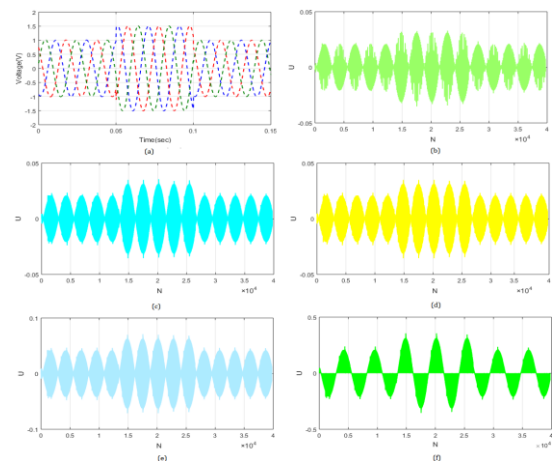


Fig. 8: Voltage swell caused by disturbances (a) 3 phase (b) Scale 1 (c) Scale 2 (d) Scale 3 (e) Scale 4 (f) Scale 5

Voltage swell caused by different scales of disturbances portrays on Figure 8. In this subplot, Fig 8(a) shows the 3-phase voltage of the DG. The voltage is balanced and unity over the interval of 0.05 to 0.1 second. Figure 8(b), the voltage increase occurs among sample points of $0-1.4 \times 10^4$ N and $2.7 \times 10^4-4 \times 10^4$ N. As the voltage on the PCC increases during islanding, the PCC voltage swells (and sags) may cause phase confusion on the frequency timeline. In the subplots Fig 8(c), the voltage increase occurs among sampling point of $0-1.4 \times 10^4$ N and $2.7 \times 10^4-4 \times 10^4$ N at scale 2. As the voltage across the PCC increases, the PCC voltage swells (and sags) may cause phase confusion on the frequency schedule. Figure 8(d) the voltage increase occurs at 3 levels between the sample point $0-1.4 \times 10^4$ N and $2.7 \times 10^4-4 \times 10^4$ N. If voltage on the PCC increases during islanding, the PCC voltage rises (and drops) may be caused by phase distortion on frequency timeline. Fig 8(e), the voltage increase occurs among sampling points of $0-1.4 \times 10^4$ N and $2.7 \times 10^4-4 \times 10^4$ N on scale 4. When the voltage on the PCC increases during islanding, the PCC voltage increases (and drops) may be caused through phase perturbation of frequency timeline. Fig 8(f) shows the voltage increase occurs at sample point of $0-1.4 \times 10^4$ N and $2.7 \times 10^4-4 \times 10^4$ N at scale 5.

5.5. Power Generation under single and multiple islanding conditions

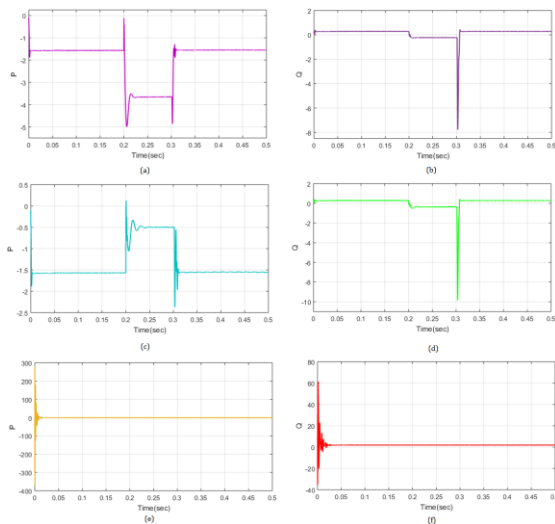


Fig 9: Performance of (a) active power P under sag (b) reactive power Q under sag (c) active power P under swell (d) reactive power Q under swell (e) active power P under harmonic (f) reactive power Q under harmonic

Figure 9 illustrates the power generation under various islanding conditions such as sag, swell and harmonic. In this graph, all active and reactive powers P and Q are generated among 0-0.5 sec. In this figure, the power P and Q is generated under sag condition which is shown in the subplot 9(a) and 9(b); here, the power P and Q is sagged

among time intervals 0.2-0.3 sec. The power P and Q is generated under swell condition which is shown in the subplot 9(c) and 9(d); here, the power P and Q is sagged among 0.2-0.3 sec. The power P and Q is generated under harmonic condition which is shown in the subplot 9(e) and 9(f). Due to this harmonics, the overall system is overheating and also caused unwanted power.

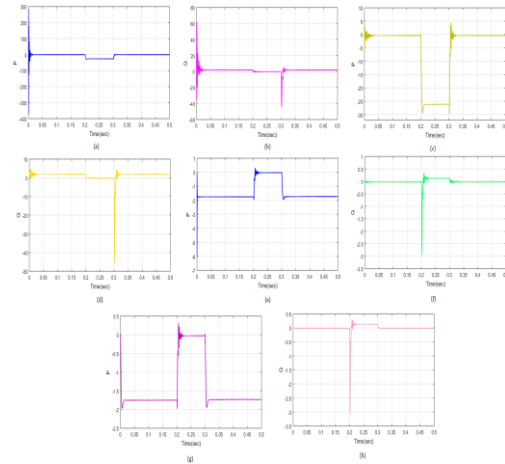


Fig 10: Performance of (a) active power P under sag-harmonic (b) reactive power Q under sag-harmonic (c) active power P under sag-transient (d) reactive power Q under sag-transient (e) active power P under swell-harmonic (f) reactive power Q under swell-harmonic (g) active power P under swell-transient (h) reactive power Q under swell-transient

Figure 10 illustrates the power generation under various multiple islanding conditions such as sag-harmonic, swell-harmonic, sag-transient and swell-transient. In this graph, all active and reactive powers P and Q generated among 0-0.5 sec. In this figure, the power P is generated under sag-harmonic and swell-harmonic condition which is shown in the subplot 10(a) and 10(e); here, the power P is sagged and swelled among 0.2-0.3 sec. The power Q is generated under sag-harmonic is sagged at 0.3 sec and the power Q is generated under swell-harmonic condition is swelled at 0.2 sec that is shown in the subplot 10(b) and 10(f). The power P and Q generated under sag-transient and swell-transient is shown in Fig 10(c), 10(d), 10(g) and 10(h).

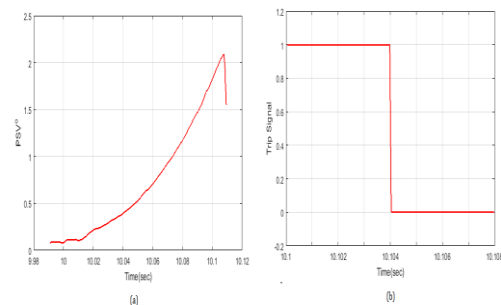


Fig. 11: Analysis of islanding event during Zero power mismatch (a) Positive Sequence Voltage VS time (b) trip signal VS time

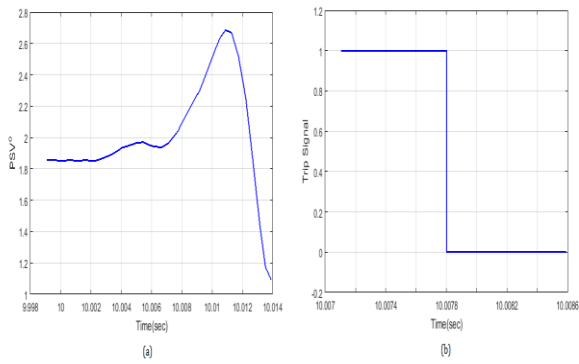


Fig. 12: Analysis of islanding event during large power mismatches (a) Positive Sequence Voltage VS time, (b) trip signal VS time

Figure 11 illustrates the analysis of islanding event during zero power situations. The maximum value of positive sequence voltage is 2.075 degree, which is shown in figure 11 (a). Here, the proposed method is used to determine the island condition and send trip signal with unit breaker of the distributed generation. The trip signal is displayed in figure 11 (b). Figure 12 illustrates the analysis of islanding event during large power mismatch. The maximum value of positive sequence voltage implies 2.7 degree, which is shown in figure 12 (a). The trip signal generated by the proposed technique is displayed on figure 12 (b).

5.6. Power generation under Non-islanding condition

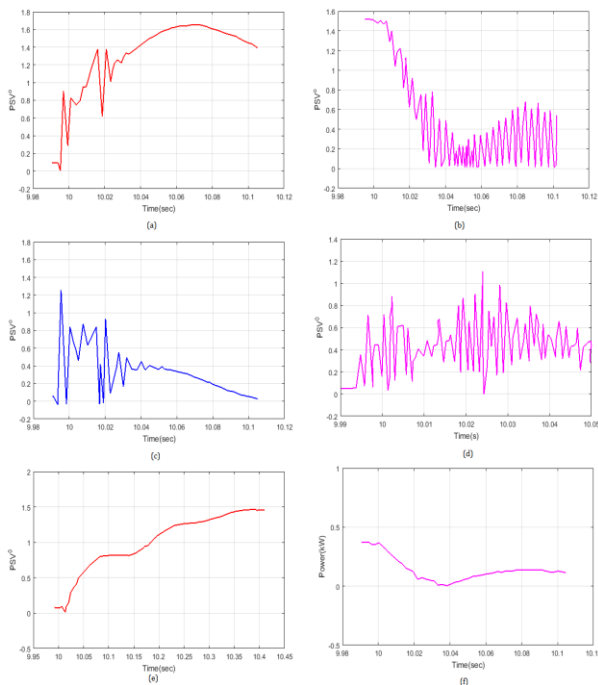


Fig. 13: Analysis of Non- islanding event (a) during load injection (b) during load ejection (c) during capacitor injection (d) during capacitor ejection (e) motor injection, (f) motor ejection

Figure 13 explains Investigation of Non- islanding event (a) during load injection (b) during load ejection(c) during capacitor injection (d) during capacitor ejection (e) motor injection, (f) motor ejection. Figure 13(a) shows that the maximal value of PSV as 1.63 degree. The trip signal generated by the proposed technique is displayed in figure 13 (b). The response of PSV and the trip signal are produced by the proposed system during this switching condition is depicted in figure 13 (c),(d). The response of PSV and the trip signal generated by the proposed technique during this motor switching condition is displayed in figure 13 (e) and (f).

5.7. Performance Analysis

The performance measures like precision, accuracy, recall, and specificity are observed. By using the proposed method, islanding phenomena are efficiently detected and categorized. The efficiency of the proposed method DMO-RFA is related to existing approaches like DFA, FF, and GSA respectively. After that, the performance parameters of proposed approach are analyzed for islanding phenomenon detection for 50 and 100 number of trials. Table 1 portrays formulas of the performance measures.

Table 1: Performance measures formula

Performance	Formulas
Accuracy	$Accuracy = \frac{T_p + T_n}{T_p + F_p + T_n + F_n}$
Precision	$Precision = \frac{T_p}{(T_p + F_p)}$
Recall	$Recall = \frac{T_p}{(T_p + F_n)}$
Specificity	$Specificity = \frac{T_n}{(F_p + T_n)}$

The island detection and classification method consists of true detection and false detection. A true detection contains either a true positive (TP) or a true negative (TN); It reflects the original signal, which is effectively expected to be either the disturbance signal or the undisturbed signal. False prediction contains false positive (FP) or false negative (FN), which involves mistaking the original signal as a disturbed or undisturbed signal. The disturbance signal is properly categorized into four classes. The current implementation of island event detection and classification is evaluated using the parameters in Table 1. Figure 14 (a) portrays performance comparison of proposed and existing

system through islanding detection for 50 numbers of trials. Table 2 portrays performance metrics like accuracy, specificity, recall and precision with existing and proposed system. Table 3 and Figure 14 (b) portrays performance comparison of proposed and existing system islanding detection for 100 numbers of trials. These results shows that the proposed DMO-RFA technique has the better accuracy than existitng methods to detect islanding and non-islanding events.

Table 2: Performance comparison of proposed and existing system through islanding condition for 50 trials

Performance Measures	DFA	FF	GSA	DMO-RFA
Accuracy	0.65	0.68	0.83	0.98
Specificity	0.64	0.82	0.88	0.93
Recall	0.72	0.86	0.96	1
Precision	0.67	0.73	0.87	0.94

Table 3: Performance comparison of proposed and existing technique through islanding condition for 100 trials

Performance	DFA	FF	GSA	DMO-RFA
Accuracy	0.64	0.76	0.87	0.96
Specificity	0.67	0.68	0.73	0.88
Recall	0.59	0.67	0.88	0.91
Precision	0.58	0.71	0.85	0.95

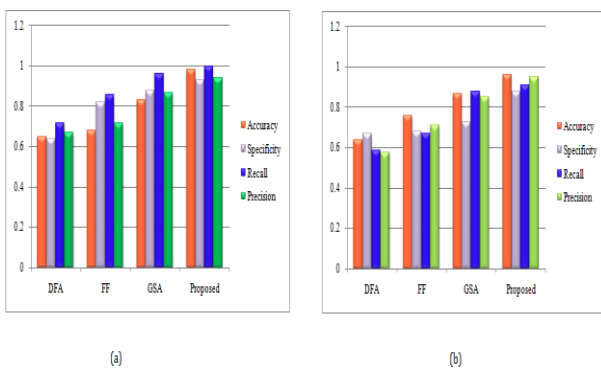


Fig. 14: Performance comparison of proposed and existing system through islanding condition for (a) 50 trials (b) 100 trials

5.8. Statistical Analysis

In the subsection, statistic measures like root mean square error (RMSE), mean absolute percentage error (MAPE), mean bias error (MBE) and consumption time are examined. By using the proposed system, islanding events

are accurately evaluated. The performance of the proposed system is related to existing systems like DFA, FF and GSA. The performance of the proposed system is determined for 50 and 100 number of trials for island detection. A statistic comparison of proposed and existing system is evaluated RMSE is the prediction error of the standard deviation. MBE captures the average bias in the prediction. MAPE is the *measure of prediction accuracy*. Table 4 portrays statistical measures formula.

Table 4: Statistical measures formula

Statistical Measures	Formulas
RMSE	$RMSE = \sqrt{\frac{1}{Z} \sum_{m=1}^Z (I_{TARGET} - I_{PREDICTED})^2}$
MAPE	$MAPE = \frac{1}{Z} \sum_{m=1}^Z \left \frac{I_{TARGET} - I_{PREDICTED}}{I_{TARGET}} \right S_n$
MBE	$MBE = \frac{1}{Z} \sum_{m=1}^Z I_{PREDICTED} - I_{TARGET}$

Where I_{TARGET} denotes target value, $I_{PREDICTED}$ refers predicted value, S_n implies number of samples per event and Z refers number of samples.

Table 5: Statistic comparison of proposed and existing technique through incipient fault for 50 trials

Model	DFA	FF	GSA	DMO-RFA
RMSE	25.3	17.8	25.6	11.2
MAPE	18	5.8	11.8	1
MBE	8.3	3.1	5.7	3
Consumption time	8.4	6.2	7.9	5

Table 6: Statistic comparison of proposed and existing technique through incipient fault for 100 rials

Model	DFA	FF	GSA	DMO-RFA
RMSE	28.3	20.5	25.7	13
MAPE	17.1	6.3	13	2.3
MBE	11	5.4	7	5.4
Consumption time	7	8	8.3	5.5

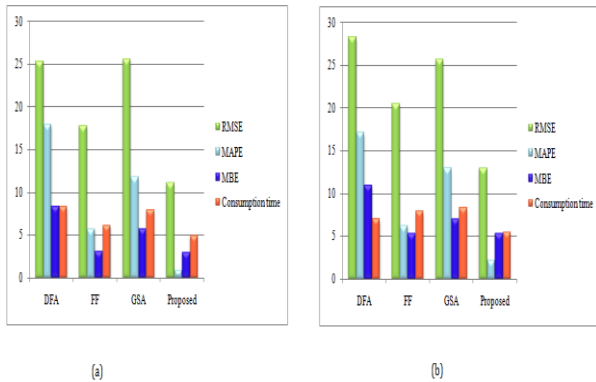


Figure 15: Statistic analysis of proposed and existing technique in (a) 50 trials (b) 100 trials

Table 5 and Figure 15 (a) portrays statistic comparison of proposed and existing system through island detection for 50 trials. Table 6 and Figure 15 (b) portrays performance comparison of proposed and existing technology through island detection for 100 number of trials. The simulation outcomes prove that proposed system may have accurate segmentation between island and dissimilar phenomena. Also, this system may overwhelm the problem of setting location limits inherent on current techniques.

6. Conclusion

A hybrid technique for island identification denotes the negative sequence voltage signal features are proposed. A passive islanding technique developed in the manuscript is highly based on the phase angle of PSV by 13 calculations of various passive indices. In the beginning, feature extraction has taken place to the negative sequence voltage signal at point of common coupling voltage then the proposed method is used to categorize and differentiate the event of islanding and non-islanding for photovoltaic generator networks coordinated with less voltage grids. Here, phase angle of positive sequence voltage includes the ability to distinguish the events of non-islanding and islanding, like fault switching, capacitor switching, induction motor switching, load switching scenarios in different situations of power mismatch. The performance of proposed method is implemented on MATLAB or SIMILINK platform and it demonstrates that the proposed system has accurate segmentation between island and various events. The simulation outcomes validate that the proposed system may have accurate segmentation amid island and dissimilar phenomena. Also, this system may conquer the problem of setting location limits inherent on current approaches. Not all island phenomena require DG disconnection. The DG generation is insufficient for local load requirements of islanded microgrid are DG disconnection important to evade power imbalance and equipment/microgrid failure. But when the generation of DGs is adequate to drive local loads and islanding phenomena are intentional, load management function may

be attained to provide uninterrupted supply to previous loads.

Reference

- [1] G. Abd-Elkader, D. F. Allam, and E. Tageldin, 2014. Islanding detection method for DFIG wind turbines using Artificial Neural Networks. *International Journal of Electrical Power & Energy Systems*, vol. 62, pp. 335–343.
- [2] P. T. Manditereza and R. Bansal, 2016. Renewable distributed generation: The hidden challenges – a review from the Protection Perspective. *Renewable and Sustainable Energy Reviews*, vol. 58, pp. 1457–1465.
- [3] S. K. G. Manikonda and D. N. Gaonkar, 2019. Comprehensive review of IDMS in DG systems. *IET Smart Grid*, vol. 2, no. 1, pp. 11–24,.
- [4] M. Mishra, S. Chandak, and P. K. Rout, 2019. Taxonomy of islanding detection techniques for distributed generation in Microgrid,. *Renewable Energy Focus*, vol. 31, pp. 9–30.
- [5] S. Bin Humayd and K. Bhattacharya, 2017. Distribution system planning to accommodate distributed energy resources and Pevs. *Electric Power Systems Research*, vol. 145, pp. 1–11.
- [6] N. Papadimitriou, V. A. Kleftakis, and N. D. Hatziaargyriou, 2015. A novel islanding detection method for microgrids based on variable impedance insertion. *Electric Power Systems Research*, vol. 121, pp. 58–66.
- [7] M. Karimi, H. Mokhlis, K. Naidu, S. Uddin, and A. H. A. Bakar, 2016. Photovoltaic penetration issues and impacts in distribution network – a review. *Renewable and Sustainable Energy Reviews*, vol. 53, pp. 594–605.
- [8] G. Bayrak and E. Kabalci, 2016. Implementation of a new remote islanding detection method for wind–solar hybrid power plants. *Renewable and Sustainable Energy Reviews*, vol. 58, pp. 1–15.
- [9] G. Bayrak, 2015. A remote islanding detection and control strategy for photovoltaic-based Distributed Generation Systems. *Energy Conversion and Management*, vol. 96, pp. 228–241.
- [10] S. J. Pinto and G. Panda, 2015. Wavelet technique based islanding detection and improved repetitive current control for reliable operation of grid-connected PV systems. *International Journal of Electrical Power & Energy Systems*, vol. 67, pp. 39–51.

- [11] H. Mohamad, H. Mokhlis, A. H. Bakar, and H. W. Ping, 2011. A review on Islanding operation and control for distribution network connected with small Hydro Power Plant. *Renewable and Sustainable Energy Reviews*, vol. 15, no. 8, pp. 3952–3962.
- [12] A. Khamis, H. Shareef, A. Mohamed and E. Bizkevelci 2015. Islanding detection in a distributed generation integrated power system using phase space technique and probabilistic neural network. *Neurocomputing*, vol. 148, pp. 587–599.
- [13] A. Rostami and N. Rezaei, 2020. A multi-feature-based passive islanding detection scheme for synchronous-machine -based distributed generation. *International Transactions on Electrical Energy Systems*, vol. 30, no. 11.
- [14] M. Heidari, G. Seifossadat, and M. Razaz, 2013. Application of decision tree and discrete wavelet transform for an optimized intelligent-based islanding detection method in distributed systems with distributed generations. *Renewable and Sustainable Energy Reviews*, vol. 27, pp. 525–532.
- [15] O. N. Faqhruldin, E. F. El-Saadany, and H. H. Zeineldin, 2014. A universal islanding detection technique for distributed generation using pattern recognition. *IEEE Transactions on Smart Grid*, vol. 5, no. 4, pp. 1985–1992.
- [16] R. Bakhshi and J. Sadeh, 2016. Voltage positive feedback based active method for islanding detection of photovoltaic system with string inverter using sliding mode controller. *Solar Energy*, vol. 137, pp. 564–577.
- [17] P. Gupta, R. S. Bhatia, and D. K. Jain, 2015. Average absolute frequency deviation value based active islanding detection technique, *IEEE Transactions on Smart Grid*, vol. 6, no. 1, pp. 26–35.
- [18] M. Al Hosani, Z. Qu, and H. H. Zeineldin, 2015. A transient stiffness measure for islanding detection of Multi-DG Systems. *IEEE Transactions on Power Delivery*, vol. 30, no. 2, pp. 986–995.
- [19] F.S. Pai and S. J. Huang, 2001. A detection algorithm for Islanding-prevention of dispersed consumer-owned storage and generating units. *IEEE Transactions on Energy Conversion*, vol. 16, no. 4, pp. 346–351.
- [20] S.-I. Jang and K.-H. Kim, 2004. An islanding detection method for distributed generations using voltage unbalance and total harmonic distortion of current. *IEEE Transactions on Power Delivery*, vol. 19, no. 2, pp. 745–752.
- [21] M. Seyedi, S. A. Taher, B. Ganji, and J. Guerrero, 2021. A hybrid islanding detection method based on the rates of changes in voltage and active power for the Multi-Inverter Systems. *IEEE Transactions on Smart Grid*, vol. 12, no. 4, pp. 2800–2811.
- [22] A. Serrano-Fontova, J. A. Martinez, P. Casals-Torrens, and R. Bosch, 2021. A robust islanding detection method with zero-non-detection zone for distribution systems with DG. *International Journal of Electrical Power & Energy Systems*, vol. 133, pp. 107247.
- [23] B. K. Choudhury and P. Jena, 2022. Superimposed impedance-based passive islanding detection scheme for DC microgrids. *IEEE Journal of Emerging and Selected Topics in Power Electronics*, vol. 10, no. 1, pp. 469–483.
- [24] O. A. Allan and W. G. Morsi, 2021. A new passive islanding detection approach using wavelets and deep learning for grid-connected photovoltaic systems. *Electric Power Systems Research*, vol. 199, pp. 107437.
- [25] A. Khair, M. Zuhaib, and M. Rihan, 2020. Effective utilization of limited channel pmus for islanding detection in a solar PV integrated distribution system. *Journal of The Institution of Engineers (India): Series B*, vol. 102, no. 1, pp. 75–86.
- [26] R. Bakhshi-Jafarabadi, J. Sadeh, E. Rakhshani, and M. Popov, 2021. High Power Quality Maximum Power Point tracking-based islanding detection method for grid-connected photovoltaic systems. *International Journal of Electrical Power & Energy Systems*, vol. 131, p. 107103.
- [27] S. V. Kulkarni, D. N. Gaonkar, and J. M. Guerrero, 2021. Operation of the microgrid with improved Droop Control Strategy and an effective islanding detection technique for automatic mode switching. *Electric Power Components and Systems*, vol. 49, no. 4-5, pp. 517–531.
- [28] A. Safdarian, M. Fotuhi-Firuzabad, M. Lehtonen, and F. Aminifar, 2015. Optimal electricity procurement in smart grids with autonomous distributed energy resources. *IEEE Transactions on Smart Grid*, vol. 6, no. 6, pp. 2975–2984.
- [29] E. A. P. Gomes, J. C. M. Vieira, D. V. Coury, and A. C. B. Delbem, 2018. Islanding detection of synchronous distributed generators using data mining complex correlations. *IET Generation, Transmission & Distribution*, vol. 12, no. 17, pp. 3935–3942.
- [30] P. Gupta, R. S. Bhatia, and D. K. Jain, 2017. Active ROCOF Relay for islanding detection. *IEEE*

- Transactions on Power Delivery*, vol. 32, no. 1, pp. 420–429.
- [31] P. Gupta, R. S. Bhatia, D. K. Jain, and Ruchika, 2018. Active islanding detection technique for distributed generation. *INAE Letters*, vol. 3, no. 4, pp. 243–250.
- [32] F. Hoke, A. Nelson, S. Chakraborty, F. Bell, and M. McCarty, 2018. An islanding detection test platform for Multi-Inverter Islands using Power Hil. *IEEE Transactions on Industrial Electronics*, vol. 65, no. 10, pp. 7944–7953.
- [33] S. Khalilpourazari and S. H. Pasandideh, 2016. Multi-item EOQ model with nonlinear unit holding cost and partial backordering: Moth-flame optimization algorithm. *Journal of Industrial and Production Engineering*, vol. 34, no. 1, pp. 42–51.
- [34] A. Khamis, H. Shareef, A. Mohamed, and E. Bizkevelci, 2015. Islanding detection in a distributed generation integrated power system using phase space technique and probabilistic neural network. *Neurocomputing*, vol. 148, pp. 587–599.
- [35] M. Ahmadipour, H. Hizam, M. L. Othman, and M. A. Radzi, 2019. Islanding detection method using Ridgelet probabilistic neural network in Distributed Generation. *Neurocomputing*, vol. 329, pp. 188–209.
- [36] H. Muda and P. Jena, 2018. Phase angle-based PC technique for islanding detection of distributed generations. *IET Renewable Power Generation*, vol. 12, no. 6, pp. 735–746.
- [37] X. Kong, X. Xu, Z. Yan, S. Chen, H. Yang, and D. Han, 2018. Deep Learning Hybrid Method for islanding detection in distributed generation. *Applied Energy*, vol. 210, pp. 776–785.
- [38] H. Laaksonen, P. Hovila, and K. Kauhaniemi, 2018. Combined islanding detection scheme utilising active network management for Future Resilient Distribution Networks. *The Journal of Engineering*, vol. 2018, no. 15, pp. 1054–1060.
- [39] H. Laaksonen, 2013. Advanced islanding detection functionality for future Electricity Distribution Networks. *IEEE Transactions on Power Delivery*, vol. 28, no. 4, pp. 2056–2064.
- [40] V. L. Merlin, R. C. Santos, A. P. Grilo, J. C. M. Vieira, D. V. Coury, and M. Oleskovicz, 2016. A new artificial neural network based method for islanding detection of distributed generators. *International Journal of Electrical Power & Energy Systems*, vol. 75, pp. 139–151.
- [41] M. ZEYBEK, 2021. Classification of UAV point clouds by Random Forest Machine Learning algorithm. *Turkish Journal of Engineering*. vol.5, no.2, pp.48-57.
- [42] P. P. Mishra and C. N. Bhende, 2018. Islanding Detection Scheme for distributed generation systems using modified Reactive Power Control Strategy. *IET Generation, Transmission & Distribution*, vol. 13, no. 6, pp. 814–820.
- [43] J. O. Agushaka, A. E. Ezugwu, and L. Abualigah, 2022. Dwarf mongoose optimization algorithm. *Computer Methods in Applied Mechanics and Engineering*, vol. 391, pp. 114570.
- [44] F. Aldosari, L. Abualigah, and K. H. Almotairi, 2022. A normal distributed dwarf mongoose optimization algorithm for global optimization and Data Clustering Applications. *Symmetry*, vol. 14, no. 5, pp. 1021.
- [45] Y. Liu, Y. Wang, and J. Zhang, 2012. New Machine Learning Algorithm: Random forest. *Information Computing and Applications*, pp. 246–252.
- [46] C.M. Rahman, and T.A. Rashid, 2019. Dragonfly algorithm and its applications in applied science survey. *Computational Intelligence and Neuroscience*.
- [47] T. Chakravorti, L. Priyadarshini, P.K. Dash and B.N. Sahu 2019. Islanding and non-islanding disturbance detection in microgrid using optimized modes decomposition based robust random vector functional link network. *Engineering Applications of Artificial Intelligence*, vol.85, pp.122-136.
- [48] M. Marzband, M. Ghadimi, A. Sumper, and J.L. Domínguez-García, 2014. Experimental validation of a real-time energy management system using multi-period gravitational search algorithm for microgrids in islanded mode. *Applied energy*, vol. 128, pp.164-174.